World Journal of Pharmaceutical and Life Sciences

Impact Factor: 7.409 www.wjpls.org Coden USA: WJPLA7

FORMULATION AND IN-VITRO EVALUATION OF NANOSPONGES CONTAINING ANTI-PIGMENTATION AGENT

Hemant[1*], Brajesh Kumar Arjariya[2], Praveen Bhawsar[3]

[1]Student Malhotra College of Pharmacy, Badwai, Near Karond, Bhopal, Madhya Pradesh.
[2]Professor Malhotra College of Pharmacy, Badwai, Near Karond, Bhopal, Madhya Pradesh.
[3]Associate Professor, Malhotra College of Pharmacy, Badwai, Near Karond, Bhopal, Madhya Pradesh.

***Corresponding Author: Hemant**

Student Malhotra College of Pharmacy, Badwai, Near Karond, Bhopal, Madhya Pradesh.

DOI: https://doi.org/10.5281/zenodo.17748815

How to cite this Article: Hemant1*, Brajesh Kumar Arjariya2, Praveen Bhawsar3 (2025). Formulation And In-Vitro Evaluation Of Nanosponges Containing Anti-Pigmentation Agent. World Journal of Pharmaceutical and Life Science, 11(12), 181–190.

Article Received on 30/10/2025 **Article Revised on 19/11/2025** **Article Published on 01/12/2025**

ABSTRACT

The present study investigates the formulating and evaluating of nanosponges containing an anti-pigmenting agent is to improve the solubility, stability, and delivery of the agent to the targeted skin cells, ultimately enhancing its efficacy in reducing skin pigmentation. The objectives include formulating stable nanosponges with high drug entrapment, characterizing their physicochemical properties, evaluating their release profile in vitro, and assessing their potential for topical delivery. The hydroquinone-loaded nanosponges exhibited a consistent physical appearance across all batches. They appeared white in color, possessed a typical odor, and maintained a solid form. The FTIR spectrum of hydroquinone was analyzed to identify its characteristic functional groups. In the present study, the zeta potential values of nanosponge formulations ranged from –0.11 mV to –15.0 mV, indicating relatively low surface charges across all formulations. Among all the evaluated formulations, Formulation F2 exhibited the most favourable particle size characteristics, with a mean particle size of 225.5 nm and a PI value of 40.2%. The observed melting point of hydroquinone was recorded at 171°C, which falls well within the established reference range of 170°C to 173°C. The pH of the hydroquinone sample was measured as 4.14, indicating a slightly acidic nature in solution. SEM is used to investigate the morphological features and surface topology of nanosponges at high resolution. The entrapment efficiency (EE %) of hydroquinone-loaded nanosponges was evaluated for five formulations (F1–F5). Among these, Formulation F2 demonstrated the highest entrapment efficiency at 92.58%, indicating superior drug encapsulation within the nanosponge matrix. These findings indicate that nanosponge-based systems can significantly enhance hydroquinone delivery, potentially improving therapeutic outcomes, reducing application frequency, and minimizing side effects in topical treatments such as for hyperpigmentation or melasma.

KEYBOARD: Nanosponge, Hydroquinone, Entrapment efficiency, Zeta potential, Hyperpigmentation, FTIR.

1. INTRODUCTION

Skin pigmentation manifests as uneven brown to dark brown spots on the skin. The onset of skin pigmentation is related to factors such as ultraviolet radiation, hormonal changes, cellular inflammation, skin damage, acne, and drug effects **(Thawabteh *et al.*, 2023).** Influenced by various factors, melanocytes undergo excessive proliferation, aggregation, and secretion of pigment, resulting in the formation of pigmentation and freckles. At present, topical chemical agents, including hydroquinone, kojic acid, retinoic acid, azelaic acid, niacinamide, vitamin C, and vitamin E, are first-line therapies for the clinical treatment of pigmentation diseases. However, most of these substances have drawbacks such as cytotoxicity, irritation, instability, or unsatisfactory therapeutic effects, which may lead to side effects and poor patient compliance **(Nautiyal and Wairkar 2021).**

Nanosponges have emerged as one of the most promising fields of science because of their perceived application in controlled drug delivery. Nanosponge delivery system can precisely control the release rates or target drugs to a specific body site and have an enormous impact on the health care system **(Shivani and Poladi 2015).** This nanosized delivery system has definite advantages for the purpose of drug delivery because of its high stability, high carrier capacity and feasibility of incorporation of both hydrophilic and hydrophobic substances. The application of nanosponges for targeted and localized delivery of therapeutic agents is the driving force for the research in this area **(Trotta *et al.*, 2014).**

Hydroquinone is a topical lightening product found in OTC products, and is used to correct skin discoloration associated with disorders of hyperpigmentation including melasma, post-inflammatory hyperpigmentation, sunspots, and freckles. It can be used alone, but is more frequently found in combination with other agents such as alpha-hydroxy acids, corticosteroids, retinoids, or sunscreen **(Saade *et al.*, 2018).** Hydroquinone has come under scrutiny due to several complications associated with its use, including dermal irritation, exogenous onchronosis, and carcinogenicity. Hydroquinone reduces melanin pigment production through inhibition of the tyrosinase enzyme, which is involved in the initial step of the melanin pigment biosynthesis pathway. Hydroquinone takes several months to take effect. Hydroquinone is used as an OTC topical lightening agent for disorders of hyperpigmentation including melasma, post-inflammatory hyperpigmentation, sunspots and freckles **(Charoo, 2022).** In this research, we focus on the Formulation and In-vitro evaluation of Nanosponges containing Anti-pigmentation agent.

2. MATERIAL AND METHODS

2.1 Chemicals

Methanol was procured from Rankem. Hydroquinone was received from Rich Pharmachem. Ethyl cellulose, DMSO and Chloroform was acquired from Sigma Aldrich. All other solvents, Chemicals and reagents used were of analytical (AR) grade and purchased from Ambika Scintific Industries**,** Lb Reagent LR Grade, Himedia laboratoris and Numex Chemical Products.

2.2 Pre-Formulation Evaluation

The purpose of pre-formulation evaluation is to systematically investigate the fundamental physical and chemical characteristics of a drug compound to provide critical information for the development of an optimal dosage form. This evaluation helps identify potential issues related to drug stability, solubility, and compatibility with excipients, which are essential for ensuring the drug's effectiveness, safety, and shelf life. By understanding these properties early, scientists can make informed decisions on the choice of formulation methods, dosage form design, and manufacturing processes. Ultimately, pre-formulation studies aim to minimize formulation challenges, reduce development time, and ensure that the final pharmaceutical product meets quality standards and therapeutic goals **(Rekha, 2011).**

2.2.1 Organoleptic Properties

The purpose of evaluating organoleptic properties is to assess the sensory attributes of a drug such as its color, taste, odor, texture, and appearance to ensure the final product is acceptable, appealing, and user-friendly for patients. **(Meltzer *et al.*, 2005).**

2.2.2. Solubility study

Solubility plays a crucial role in pharmaceutical development, directly impacting a drug's absorption, bioavailability, and therapeutic effectiveness. This qualitative evaluation provided initial insights into the drug's solubility behaviour, aiding in the rational selection of solvents for further formulation development and compatibility studies **(Stielow *et al.*, 2023).**

2.2.3 Melting Point

To determine the melting point of Hydroquinone, a small amount of the finely powdered drug is packed into a capillary tube sealed at one end **(Chen *et al.*, 2005).**

2.2.4 Determination of Lambda max and calibration curve

1. Lambda (λ) max determination

The purpose of determining the Lambda (λ) max of Hydroquinone is to identify the specific wavelength at which the compound shows maximum absorbance in the UV-visible spectrum. This wavelength is critical for conducting accurate and sensitive quantitative analyses, such as the preparation of calibration curves and the estimation of drug concentration in formulations. Using the λ max ensures optimal sensitivity and minimizes analytical errors during spectrophotometric measurements. It also helps in selecting appropriate analytical conditions for routine quality control and stability studies **(Ravi *et al.*, 2020).**

2. Standard calibration curve

The construction of a standard calibration curve is essential for the quantitative analysis of Hydroquinone using UV-visible spectrophotometry. By correlating known concentrations of the analyte to their respective absorbance values at the compound's characteristic λ max, a linear regression model can be established. This model facilitates the determination of unknown sample concentrations through interpolation. The calibration curve also serves as a validation tool, providing critical parameters such as linearity, sensitivity, and detection limits. Accurate calibration is indispensable for ensuring the precision and accuracy of analytical measurements, which underpin quality control, formulation development, and stability studies in pharmaceutical research **(Ourique *et al.*, 2012).**

2.2.5 Preparation of calibration curve

An initial stock solution of Hydroquinone was prepared and serially diluted with the appropriate solvent to obtain a series of working standards at concentrations of 10, 20, 30, 40, and 50 µg/mL. The absorbance of each diluted solution was measured against a solvent blank using UV-visible spectrophotometry. A calibration curve was then constructed by plotting Hydroquinone concentration on the X-axis against the measured absorbance on the Y-axis. This curve, covering the concentration range of 10 to 50 µg/mL, was assessed for linearity in accordance with Beer-Lambert's law, ensuring its suitability for accurate quantitative analysis of unknown samples **(Kumar and Kumar 2021).**

2.2.6 Fourier transmission Infra-Red Spectroscopy

The FT-IR spectra of pure Hydroquinone was recorded over the range of 4000 to 400 cm^{-1} using the KBr pellet method on an FT-IR spectrophotometer. To prepare the pellet, 1 mg of the sample (Hydroquinone) was thoroughly mixed with 100 mg of spectroscopic-grade potassium bromide (KBr), which had been pre-dried under an infrared lamp. This mixture was then compressed using a hydraulic press to form a transparent disc, which was placed in the sample holder of the FT-IR instrument for spectral recording. The purpose of this analysis is to identify and characterize the functional groups present in Hydroquinone and to detect any possible interactions between the drug and excipients **(Jia *et al.*, 2024).**

2.3 Formulation of Hydroquinone -loaded nanosponges

Drug loaded Nanosponges were prepared by the emulsion solvent evaporation technique using the drug (Hydroquinone) 4% and polyvinyl alcohol (PVA) 0.1 to 0.3%, w/v, compositions of formulations were tabulated in Table 4. Briefly, organic phase was prepared by dissolving ethyl cellulose (EC) (100–500 mg) and drug in 20 mL dichloromethane (DCM). Separately, an aqueous phase was prepared composed of (0.1 to 0.3%, w/v) PVA in 100 mL of deionized water. Thereafter, the organic phase was emulsified drop wise into the aqueous phase by sonication, for 10 to 30 min. The formed NS was stabilized by PVA, which avoid particle agglomerations. Thereafter, the dispersion was kept on thermostatically controlled magnetic stirrer with continuous stirring for 3 h. After complete evaporation of the organic solvent, the drug loaded nanosponges were washed three times.

Table 1: Composition of Nano sponges' formulation.

Formulation Code	Ethyl cellulose (mg)	PVA (%)	Drug hydroquinone (%)	DCM (ml)	Stirring time (Min.)	Sonication time (Min.)	Distilled water (ml)
(Nano sponges) F1	100	0.5	4.0	20	30	10	100
(Nano sponges) F2	200	0.4	4.0	20	30	10	100
(Nano sponges) F3	300	0.3	4.0	20	30	10	100
(Nano sponges) F4	400	0.2	4.0	20	30	10	100
(Nano sponges) F5	500	0.1	4.0	20	30	10	100

2.4 Evaluation parameter of nanosponges

2.4.1 Physical Appearance of Nanosponges

The physical appearance of the nanosponges was assessed through visual inspection, focusing on attributes such as color, texture, and homogeneity **(Darandale and Vavia 2013).**

2.4.2 Particle size

The nanosponge particle size was characterized utilizing dynamic light scattering (DLS) technology on a Malvern Zetasizer instrument **(Mashaqbeh Mashaqbeh *et al.*, 2021).**

2.4.3 Zeta potential analysis

The purpose of measuring the zeta potential of nanosponges is to evaluate their surface charge, which is a key indicator of the physical stability of the suspension. The prepared dispersion was then placed into a zeta potential cell and analyzed using a Malvern Zetasizer. **(Penjuri *et al.*, 2016).**

2.4.4 Scanning Electron Microscopic (SEM)

The primary objective of employing Scanning Electron Microscopy (SEM) is to meticulously examine the surface morphology and structural integrity of Hydroquinone-loaded nanosponges, providing insights into their nano structural characteristics **(Rydz *et al.*, 2019).**

2.4.5 Entrapment efficiency

The primary objective of determining the entrapment efficiency (EE) of Hydroquinone-loaded nanosponges is to assess the extent to which the drug is encapsulated within the nanosponges, providing insight into the formulation's drug-loading capacity and potential therapeutic efficacy. The absorbance was measured at the appropriate wavelength corresponding to Hydroquinone's maximum absorbance. The entrapment efficiency was calculated using the formula:

Entrapment Efficiency (%) = (Amount of drug entrapped / Total amount of drug added) × 100

2.5 *In-vitro* drug release study

The dialysis bag diffusion method was employed to look into the drug release in vitro of Nanosponges compositions. A dialysis bag was filled with the Nano sponges formulation and then put in a beaker containing 100 milliliters of phosphate buffer with a pH of 7.4. The beaker was placed over a magnetic stirrer to maintain the assembly's temperature at 37 ± 2 °C during the

experiment. During the trial, the speed remained fixed at 100 rpm. At certain intervals, samples (2 ml) were taken out and swapped out with equal volumes of brand-new pH 7.4 phosphate buffers. A UV-visible spectrophotometer was used to analyze the samples at 293.0 nm after the proper dilutions. Several kinetic models were employed to characterize the release kinetics in order to interpret the in vitro drug release data. **(Bohrey et al., 2016).**

Zero order kinetics
First order kinetics
Higuchi's Model
Korsmeyer-Peppas model

3. RESULT AND DISCUSSION

3.1 Pre-formulation study of Hydroquinone

3.1.1 Organoleptic evaluation

The organoleptic evaluation of hydroquinone showed consistent color, odor, and texture, indicating good physical stability and quality of the sample.

Table 2: Organoleptic evaluation of Hydroquinone.

Drug	Organoleptic properties	Observation
Hydroquinone	Color	Off White crystals
	Odor	Odorless
	Appearance	Crystalline
	State	Solid

3.1.2 Solubility study

Table 3: Solubility study of Hydroquinone.

Drug	Solvents	Observation/Inference
Hydroquinone	Water	Sparingly soluble
	Ethanol	Freely soluble
	Methanol	Freely soluble
	Chloroform	Sparingly soluble
	DMSO	Soluble
	PBS -7.4 pH	Freely soluble

3.1.3 Determination of pH and melting point

Table 4: Determination of pH and melting point of Hydroquinone.

Drugs	Observed (pH)	Reference (pH)	Observed (Melting Point)	Reference (Melting Point)
Hydroquinone	4.1	3.0 to 5.5	171°C	170°C to 173°C

3.1.4 Determination of λ max by UV spectroscopy of drug

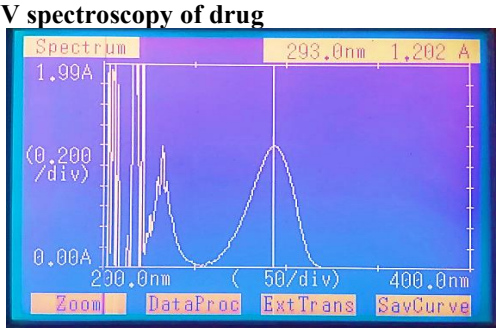

Graph 1:- UV graph of Hydroquinone (293.0 nm).

3.1.5 Standard calibration curve

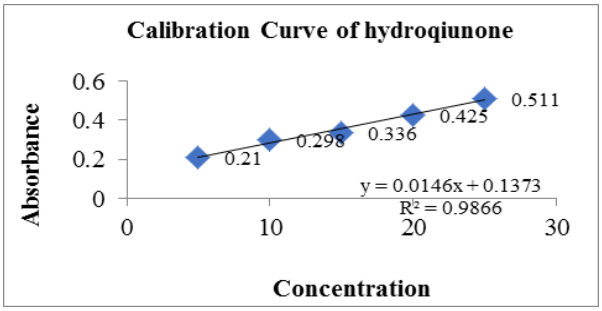

Graph 2: Calibration curve of hydroquinone.

The regression equation was developed by graphing the absorbance versus hydroquinone concentration from 5 to 25µg/ml. A 5-point calibration curve was generated for drug concentrations from 5 to 25µg/ml.

3.2 Functional group identified by Infra-Red spectroscopy

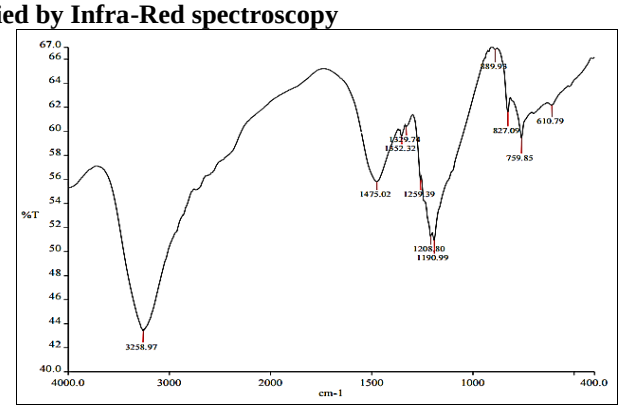

Graph 3:- FTIR study of Hydroquinone.

Table 5: Interpretation of IR spectrum of Hydroquinone.

Peak obtained	Reference peak	Functional group	Name of functional group
3258.97	3550-3200	O–H stretching	Alcohols
1352.32	1372-1335	S=O stretching	Sulfonate
1259.39	1275-1200	C-O stretching	Alkyl aryl ether
1190.99	1205-1124	C-O stretching	Tertiary alcohol
827.09	840-790	C=C bending	Alkene
759.85	850-550	C-Cl stretching	Halo compound
610.79	690-515	C-Br stretching	Halo compound

3.3 Characterization of Hydroquinone loaded Nanosponges formulation

3.3.1 Physical Appearance of Nanosponges

Table 6: Physical Appearance of Nanosponges.

Formulation	Parameters	Observation
Nanosponges	Colour	Off White
	Odour	Characteristic
	Appearance	Solid

3.3.2 Particle Size analysis

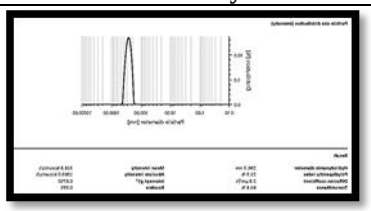

Graph 4: Particle size (F1)

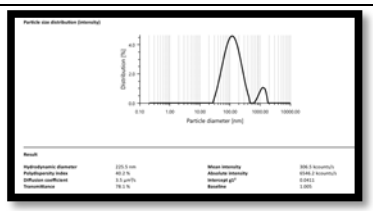

Graph 5: Particle size (F2)

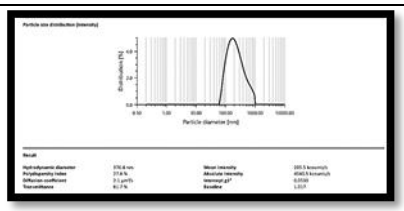

Graph 6: Particle size (F3)

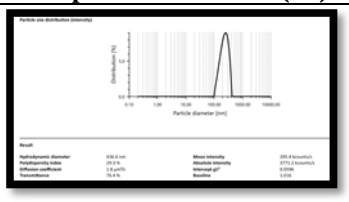

Graph 7: Particle size (F4)

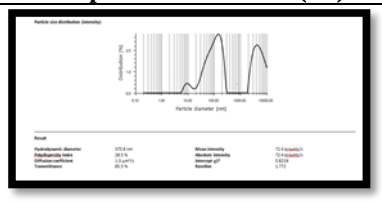

Graph 8: Particle size (F5)

Table 7: Particle size of Nano sponges.

Formulation code	Particle size (nm)	PI Value %
(Nano sponges) F1	286.3	22.9
(Nano sponges) **F2**	**225.5**	**40.2**
(Nano sponges) F3	376.8	27.8
(Nano sponges) F4	436.6	29.3
(Nano sponges) F5	375.8	85.5

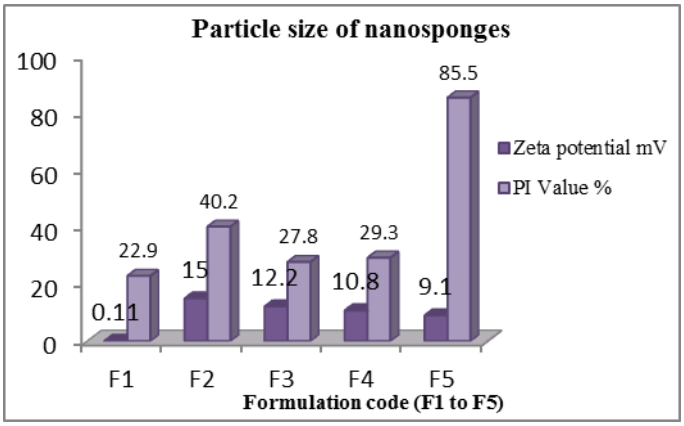

Graph 9: graphical representation of particle size of nanosponges.

Among all the evaluated formulations, Formulation F2 exhibited the most favourable particle size characteristics, with a mean particle size of 225.5 nm and a PI value of 40.2%. This nanoscale size range is optimal for enhancing drug solubility, skin penetration (for topical use), and controlled release.

3.3.3 Zeta potential analysis

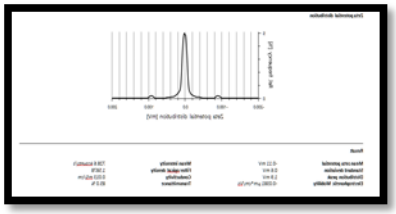

Graph 10: Zeta potential (F1)

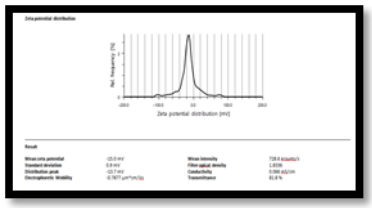

Graph 11: Zeta potential (F2)

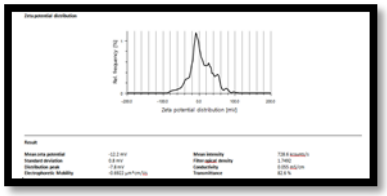

Graph 12: Zeta potential (F3)

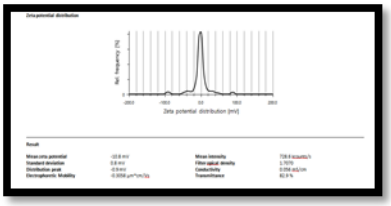

Graph 13: Zeta potential (F4)

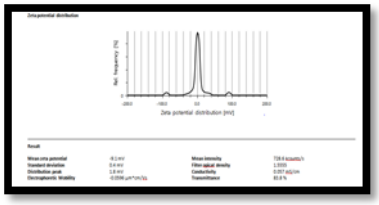

Graph 14: Zeta potential (F5)

Table 8: Zeta potential of nanosponges.

Formulation Code	Zeta potential mV
(Nano sponges) F1	-0.11
(Nano sponges) **F2**	**-15.0**
(Nano sponges) F3	-12.2
(Nano sponges) F4	-10.8
(Nano sponges) F5	-9.1

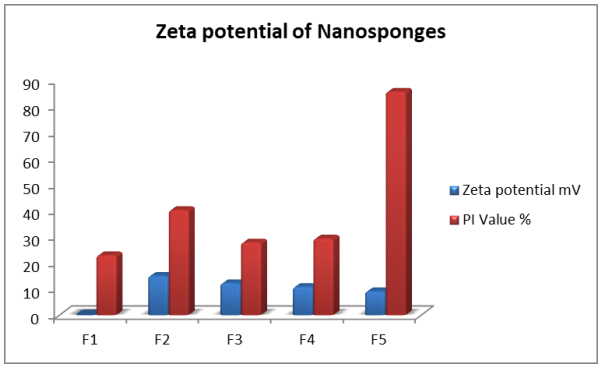

Graph 15: graphical representation of Zeta potential of nanosponges.

NPs F1 exhibited the lowest zeta potential (–0.11 mV), suggesting a near-neutral surface charge. This could lead to poor colloidal stability, increasing the likelihood of particle aggregation. NPs F2 showed the highest negative zeta potential (–15.0 mV), implying better stability compared to other formulations, but still not within the ideal range for optimal electrostatic stabilization.

3.3.4 Scanning electron microscope (SEM)

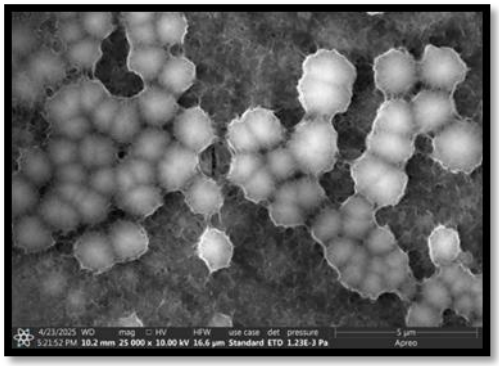

Figure 25: Scanning electron microscope (SEM).

3.3.5 Entrapment efficacy

Table 9: Entrapment efficacy.

Formulations (F1-F5)	Entrapment efficacy (%)
(Nano sponges) F1	81.30
(Nano sponges) **F2**	**92.58**
(Nano sponges) F3	80.23
(Nano sponges) F4	79.46
(Nano sponges) F5	75.65

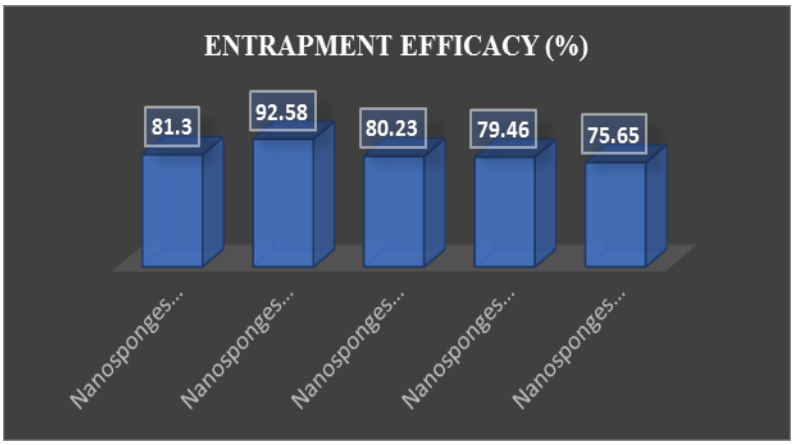

Graph 16: Graphical representation of Entrapment efficacy.

3.4 *In-vitro* drug release

Table 10: Release kinetics study of optimized Nanosponges formulation.

Time (Hr)	Cumulative % drug released	% Drug remaining	Square root time	log Cumu % drug remaining	log time	log Cumu % drug released
0	0	100	0.000	2.000	0.000	0.000
2	22.12	77.88	1.414	1.891	0.301	1.345
4	34.2	65.8	2.000	1.818	0.602	1.534
6	45.15	54.85	2.449	1.739	0.778	1.655
8	58.23	41.77	2.828	1.621	0.903	1.765
10	68.88	31.12	3.162	1.493	1.000	1.838
12	79.98	20.02	3.464	1.301	1.079	1.903
14	87.65	12.35	3.742	1.092	1.146	1.943
15	97.97	2.03	3.873	0.307	1.176	1.991

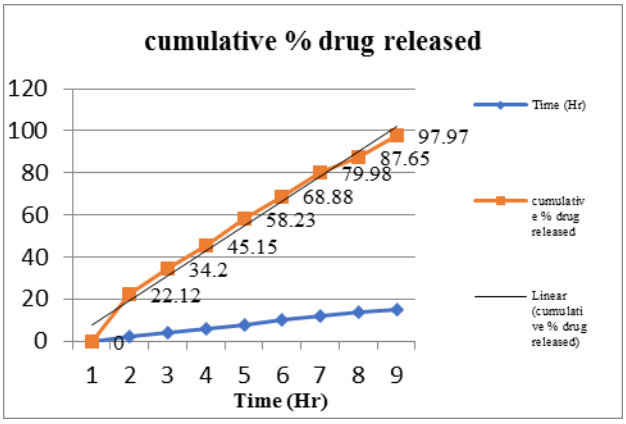

Graph 17: cumulative percentage drug released study.

Table 10: R-square values and rate constants of release kinetics of nanosponges (Correlation value (R2 value)

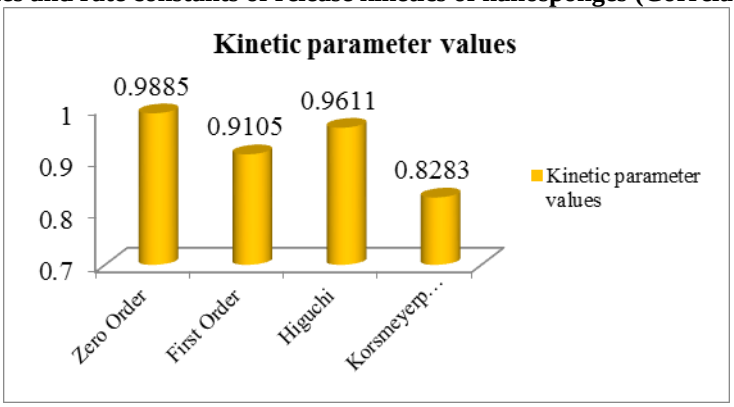

Graph 18: Graphical representation of all models

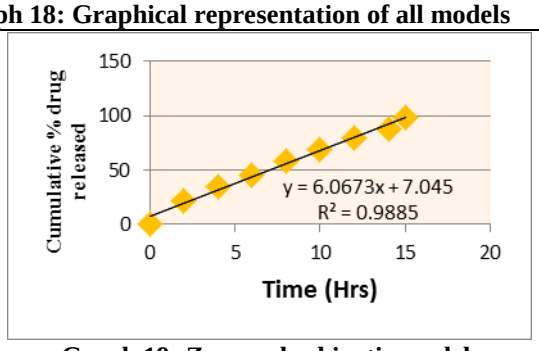

Graph 19: Zero order kinetic model.

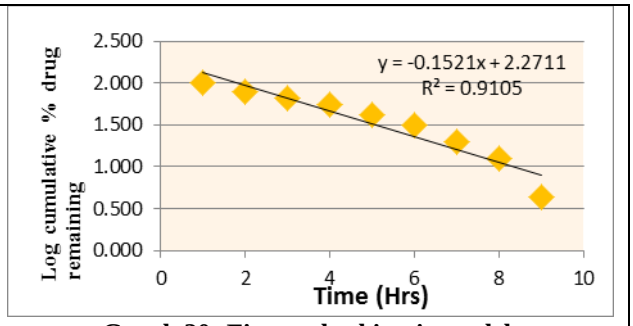

Graph 20: First order kinetic model.

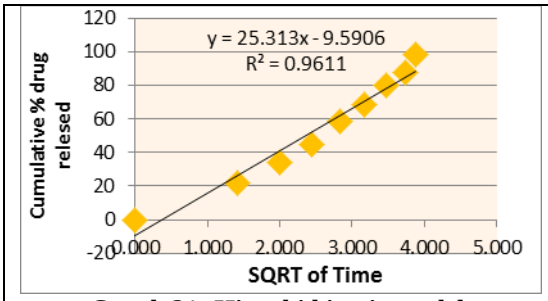

Graph 21: Higuchi kinetic model.

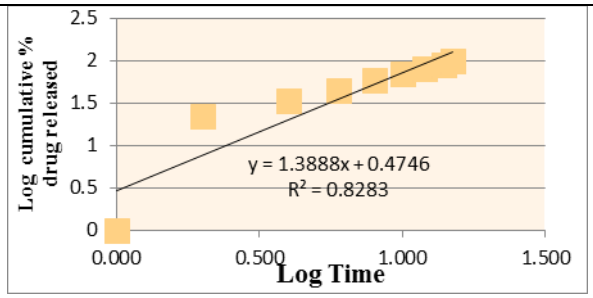

Graph 22: Kosmeuyar pappas kinetic model.

To understand the mechanism of drug release, various kinetic models were applied to the release data. The corresponding R^2 values help determine the best-fit model: R^2 Value: Zero Order- 0.9885 (Best fit), First Order- 0.9105, Higuchi -0.9611 and Korsmeyer-Peppas- 0.8283 Zero-Order Model (R^2 = 0.9885): Indicates that the drug is released at a constant rate, independent of concentration. Best-fit model, suggesting that the nanosponge formulation achieves a controlled release system This is desirable for maintaining consistent therapeutic drug levels. First-Order Model (R^2 = 0.9105): Implies concentration-dependent drug release. The lower R^2 compared to Zero-order indicates this model does not adequately describe the release kinetics for this formulation. Higuchi Model (R^2 = 0.9611): Suggests that the release is diffusion-controlled, consistent with the structure of nanosponges (porous matrix). The high R^2 value supports that Fickian diffusion plays a significant role in the release mechanism. Korsmeyer-Peppas Model (R^2 = 0.8283): Less reliable due to lower R^2. If the release exponent (n) were available, we could determine whether the release follows Fickian or non-Fickian (anomalous) transport. However, the low R^2 implies this model does not best represent the system. The optimized nanosponge formulation exhibits a controlled and sustained drug release, achieving nearly 98% release over 15 hours. The Zero-order model (R^2 = 0.9885) best fits the release profile, indicating a constant and predictable release rate ideal for therapeutic use. The high Higuchi R^2 also confirms a significant role of diffusion in the release process. These results confirm that the nanosponges are effectively engineered to offer prolonged release, reduce dosing frequency, and potentially improve patient compliance.

4. CONCLUSION

The results of this study demonstrate that hydroquinone-loaded nanosponges can be successfully formulated using suitable excipients and processing conditions. Formulation F2 showed superior physicochemical characteristics, including small and uniform particle size, high entrapment efficiency, and excellent zeta potential, all of which are critical for effective and stable drug delivery.

The stable performance of the optimized formulation under ICH-recommended conditions further confirms its suitability for pharmaceutical development, especially for topical applications where hydroquinone is commonly used for hyperpigmentation disorders. Thus, this nanosponge-based delivery system provides a promising and innovative platform for improving the therapeutic efficacy and shelf life of hydroquinone in future dermatological formulations.

These findings indicate that nanosponge-based systems can significantly enhance hydroquinone delivery, potentially improving therapeutic outcomes, reducing application frequency, and minimizing side effects in topical treatments such as for hyperpigmentation or melasma.

5. REFERENCES

1. Thawabteh, A. M., Jibreen, A., Karaman, D., Thawabteh, A., & Karaman, R. (2023). Skin pigmentation types, causes and treatment—a review. *Molecules*, *28*(12): 4839.
2. Nautiyal, A., & Wairkar, S. (2021). Management of hyperpigmentation: Current treatments and emerging therapies. *Pigment cell & melanoma research*, *34*(6): 1000-1014.
3. Shivani, S., & Poladi, K. K. (2015). Nanosponges-novel emerging drug delivery system: A review. *International journal of pharmaceutical sciences and research*, *6*(2): 529.
4. Trotta, F., Dianzani, C., Caldera, F., Mognetti, B., & Cavalli, R. (2014). The application of nanosponges to cancer drug delivery.
5. Saade, D. S., Maymone, M. B., Secemsky, E. A., Kennedy, K. F., & Vashi, N. A. (2018). Patterns of over-the-counter lightening agent use among patients with hyperpigmentation disorders: a United States-based cohort study. *The Journal of Clinical and Aesthetic Dermatology*, *11*(7): 26.
6. Charoo, N. A. (2022). Hyperpigmentation: looking beyond hydroquinone. *Journal of Cosmetic Dermatology*, *21*(10): 4133-4145.
7. Rekha, S., Upadhyay, D., Bhattacharya, A., Kooijman, E., Goon, S., Mahato, S., & Pant, N. C. (2011). Lithostructural and chronological constraints for tectonic restoration of Proterozoic accretion in the Eastern Indian Precambrian shield. *Precambrian Research*, *187*(3-4): 313-333.
8. Meltzer, D. E. (2005). Relation between students' problem-solving performance and representational format. *American journal of physics*, *73*(5): 463-478.

9. Stielow, M., Witczyńska, A., Kubryń, N., Fijałkowski, Ł., Nowaczyk, J., & Nowaczyk, A. (2023). The bioavailability of drugs—the current state of knowledge. *Molecules*, *28*(24): 8038.
10. Willis, S. N., Chen, L., Dewson, G., Wei, A., Naik, E., Fletcher, J. I., ... & Huang, D. C. (2005). Proapoptotic Bak is sequestered by Mcl-1 and Bcl-xL, but not Bcl-2, until displaced by BH3-only proteins. *Genes & development*, *19*(11): 1294-1305.
11. Ravi, R. C. (2020). Lockdown of colleges and universities due to COVID-19: Any impact on the educational system in India?. *Journal of education and health promotion*, *9*(1): 209.
12. Ourique, A. F., Contri, R. V., Guterres, S. S., Beck, R. C. R., Pohlmann, A. R., Melero, A., & Schaefer, U. F. (2012). Set-up of a method using LC-UV to assay mometasone furoate in pharmaceutical dosage forms. *Quimica Nova*, *35*: 818-821.
13. Kumar, A. P., & Kumar, D. (2021). Determination of pharmaceuticals by UV-visible spectrophotometry. *Current Pharmaceutical Analysis*, *17*(9): 1156-1170.
14. Jia, N., Luo, X., Fang, Z., & Liao, C. (2024). When and how artificial intelligence augments employee creativity. *Academy of Management Journal*, *67*(1): 5-32.
15. Darandale, S. S., & Vavia, P. R. (2013). Cyclodextrin-based nanosponges of curcumin: formulation and physicochemical characterization. *Journal of inclusion phenomena and macrocyclic chemistry*, *75*: 315-322.
16. Mashaqbeh, H., Obaidat, R., & Al-Shar'i, N. (2021). Evaluation and characterization of curcumin-β-cyclodextrin and cyclodextrin-based nanosponge inclusion complexation. *Polymers*, *13*(23): 4073.
17. Penjuri, S. C. B., Ravouru, N., Damineni, S., Bns, S., & Poreddy, S. R. (2016). Formulation and evaluation of lansoprazole loaded Nanosponges. *Turk J Pharm Sci*, *13*(3): 304-310.
18. Rydz, J., Šišková, A., & Andicsová Eckstein, A. (2019). Scanning electron microscopy and atomic force microscopy: topographic and dynamical surface studies of blends, composites, and hybrid functional materials for sustainable future. *Advances in Materials Science and Engineering*, *2019*(1): 6871785.
19. Tai, D. B. G., Shah, A., Doubeni, C. A., Sia, I. G., & Wieland, M. L. (2021). The disproportionate impact of COVID-19 on racial and ethnic minorities in the United States. *Clinical infectious diseases*, *72*(4): 703-706.
20. Bohrey, S., Chourasiya, V., & Pandey, A. (2016). Polymeric nanoparticles containing diazepam: preparation, optimization, characterization, in-vitro drug release and release kinetic study. Nano Convergence, 3(1): 3.